Final Draft
of the original manuscript:

Ateghang, B.; Wartenberg, M.; Gassmann, M.; Sauer, H.:
Regulation of cardiotrophin-1 expression in mouse embryonic stem cells by HIF-1{alpha} and intracellular reactive oxygen species
In: Journal of Cell Science (2006) Company of Biologists Limited

DOI: 10.1242/jcs.02798

REGULATION OF CARDIOTROPHIN-1 (CT-1) EXPRESSION IN MOUSE EMBRYONIC STEM CELLS BY HYPOXIA AND INTRACELLULAR REACTIVE OXYGEN SPECIES

[#]Bernadette Ateghang, [§]Maria Wartenberg, [&]Max Gassmann and [#]Heinrich Sauer

From the [#]Department of Physiology, University Giessen, Germany;
[§]GKSS Research Institute, Department of Cell Biology, Teltow, Germany;
[&]Institute of Veterinary Physiology, Vetsuisse Faculty, University of Zurich, Switzerland

Running Title: Redox regulation of Cardiotrophin-1

Address correspondence to: Heinrich Sauer, Department of Physiology, Justus-Liebig-University Gießen, Aulweg 129, 35392 Gießen, Germany, phone: +49 (0) 641-9947333; fax: +49 (0) 641-9947219; E-mail: heinrich.sauer@physiologie.med.uni-giessen.de

Cardiomyogenesis of mouse embryonic stem (ES) cells is promoted by CT-1, which is a member of the IL-6 interleukin superfamily and acts through the tall gp130 cytokine receptor. The regulation of CT-1 expression in ES cells is unknown, however. Herein it is shown that prooxidants (menadione, hydrogen peroxide) as well as chemical ($CoCl_2$) and physiological (1% O_2) hypoxia significantly increased CT-1 as well as HIF-1α protein and mRNA expression in ES cell-derived embryoid bodies, indicating that CT-1 expression is regulated by reactive oxygen species (ROS) and hypoxia. Treatment with either prooxidants or chemical hypoxia increased gp130 phosphorylation and protein expression of NADPH-oxidase subunits p22-phox, p47-phox, p67-phox, as well as *Nox-1* and *Nox-4* mRNA. Consequently, inhibition of NADPH-oxidase activity by diphenylen iodonium chloride (DPI) and apocynin abolished prooxidant- and chemical hypoxia-induced upregulation of CT-1. Prooxidants and chemical hypoxia activated mitogen-activated protein kinases (MAPKs) ERK1,2, JNK and p38 as well as PI3-kinase. The proxidant and $CoCl_2$-mediated upregulation of CT-1 was significantly inhibited in the presence of the ERK1,2 antagonist UO126, the JNK antagonist SP600125, the p38 antagonist SKF86002, the PI3-kinase antagonist LY294002, the Jak-2 antagonist AG490 as well as in the presence of free radical scavengers. In HIF-1α$^{-/-}$ ES cells cardiomyogenesis was completely absent. Furthermore, in HIF-1α$^{-/-}$ ES cells prooxidants as well as chemical hypoxia failed to upregulate CT-1 expression. Our data demonstrate that CT-1 expression in ES cells is regulated by ROS and HIF-1α and support a role of CT-1 in survival and proliferation of ES cell-derived cardiac cells.

The cytokine CT-1 is a member of the IL-6 family of cytokines acting through a heterodimer of the LIFR*ß* and gp130 which become tyrosine phosphorylated by Janus kinases (Jaks) since neither gp130 nor LIFR*ß* contain inherent kinase activity. The Jaks activate multiple downstream signalling pathways which involve signal transducers and activators of transcription (STATs), MAPKs, PI3-kinase and NF-κB (1;2). Several biological effects with vital importance on heart development and function have been attributed to CT-1. In embryonic and neonatal cardiomyocytes CT-1 has been demonstrated to mediate cell proliferation and support cell survival (3). In ES cells CT-1 has been recently shown to stimulate cardiomyogenic differentiation and cell proliferation by a mechanism involving ROS as signalling molecules in Jak/STAT-, MAPK-, and NF-κB-mediated signal transduction cascades (4). Besides its important function in embryonic and neonatal tissues CT-1 exerts protective function in the adult heart by inducing cell hypertrophy through stimulation of sarcomer assembly in series with subsequent increase in cardiomyocyte cell length (5), and by preventing apoptosis in vitro and in vivo (6). Furthermore, CT-1 has been shown to stimulate cardiac fibroblast proliferation and migration, thereby allowing repopulation of scars developing after cardiac infarction with cells which promote wound healing and preserve cardiac function (7).

The molecular regulation of CT-1 expression is so far largely unknown. The properties of CT-1 as a cardioprotective cytokine in stress conditions predicts upregulation during cardiac diseases which are characterized by an

environment of hypoxia, inflammation and oxidative stress. It could be hypothesized that stress stimuli occurring during cardiac diseases regulate the expression of CT-1 which subsequently exerts its cardioprotective effect. In this respect it has been demonstrated that CT-1 is cardioprotective for ischemia-reperfusion injury, even when added at the point of reoxygenation (8;9), and it was discussed that early expression of CT-1 in the ischemic myocardium may represent an adaptive, protective phenomenon that is beneficial in reducing myocyte loss and inducing hypertrophy of remaining myocytes, thereby allowing to maintain overall ventricular function (1). Indeed elevated serum levels of CT-1 have been observed in patients with unstable angina pectoris (10), acute myocardial infarction (7;11) and heart failure (11). A comparable microenvironment of hypoxia and elevated ROS generation may prevail in the heart of the early postimplantation embryo and may regulate CT-1 expression in the embryonic heart. Hypoxia and robust endogenous ROS production have been previously shown to occur in differentiating ES cells and may represent one key stimulus for regulation of CT-1 expression as well as induction of the cardiomyogenic cell lineage (12).

The current study was undertaken to evaluate the impact of the stress factors hypoxia and ROS on the signalling cascades resulting in CT-1 expression. The ES cell model was chosen since it allows the analysis of molecular mechanisms of cardiomyogenic differentiation as well as the study of gene function in homozygous knockouts of genes resulting in early embryonic lethality. Our data point out that hypoxia as well as ROS employ a common HIF-1α-regulated signalling pathway which results in increased CT-1 expression. Comparable situations of hypoxia and oxidative stress occur in various stress conditions and presumably mediate cardioprotection as well as cardiac cell proliferation and hypertrophy by CT-1 in the embryonic and adult heart.

Materials and Methods

Materials - N-(2-mercapto-propionyl)-glycine NMPG, 2-methoxyestradiol (2-ME), diphenylene iodonium chloride (DPI) and apocynin were purchased from Sigma, Deisenhofen, Germany. Trolox (water-soluble vitamin E), UO126, SP600125, SKF86002, LY294002 and AG490 were from Calbiochem (Bad Soden, Germany).

Spinner-culture technique for cultivation of embryoid bodies - The ES cell line CCE as well as the ES cell lines HM-1 wildtype (wt) and HM-1 homozygous deficient for HIF-1α (HIF-1$\alpha^{-/-}$) (13) were grown on mitotically inactivated feeder layers of primary murine embryonic fibroblasts for a maximum of eight passages in Iscove's medium (Gibco, Live Technologies, Helgerman Court, MD, USA) supplemented with 18% heat-inactivated (56°C, 30 min) foetal calf serum (FCS) (Sigma), 2 mM Glutamax, (PAA, Cölbe, Germany), 100 µM β-mercaptoethanol (Sigma, Deisenhofen, Germany), 1% (v/v) NEA non-essential amino acids stock solution (100 x) (Biochrom), 0.8% (v/v) MEM amino acids (50x) (Biochrom), 1mM Na^+-pyruvate (Biochrom), 0.25% (v/v) penicillin/streptomycin (200 x) (Biochrom) and 1000 U/ml LIF (Chemicon, Hampshire, UK) in a humidified environment containing 5% CO_2 at 37°C, and passaged every 2-3 days. At day 0 of differentiation adherent cells were enzymatically dissociated using 0.2% trypsin and 0.05% EDTA in phosphate-buffered saline (PBS) (Gibco), and seeded at a density of $1 \cdot 10^7$ cells ml^{-1} in 250 ml siliconized spinner flasks (Integra Biosciences, Fernwald, Germany) containing 100 ml Iscove's medium supplemented with the same additives as described above. Following 24 hours 150 ml medium was added to give a final volume of 250 ml. The spinner flask medium was stirred at 20 r.p.m. using a stirrer system (Integra Biosciences), and 150 ml cell culture medium was exchanged every day.

Immunohistochemistry - Immunohistochemistry was performed with whole mount embryoid bodies. As primary antibodies a rat anti-mouse CT-1 monoclonal antibody (1:100) (R&D Systems, Wiesbaden, Germany), a mouse anti-mouse HIF-1α monoclonal antibody (1:100) (R&D Systems), a goat anti-mouse gp130 antibody (1:100) (R&D Systems), a phosphospecific polyclonal goat anti-mouse p-gp130 antibody (1:100) (Santa Cruz Biotechnologies, Santa Cruz, CA), polyclonal goat anti-mouse Mox-1 (Nox-1), Nox-4, p22-phox, p47-phox, p67-phox antibodies (1:50) (all from Santa Cruz), rabbit polyclonal anti-ERK1,2, anti-JNK, anti-p38 and PI3-kinase P85 antibodies (1:50) directed against the active (phosphorylated) form of the proteins (all from New England Biolabs, Frankfurt, Germany), were used. For HIF-1α, CT-1, gp130, p-gp130, Mox-1, Nox-4, p22-phox, p-67-phox staining

the respective tissues were fixed in ice-cold methanol for 30 min at -20°C, and washed with PBS containing 0.1% Triton X-100 (PBST) (Sigma). For PI3-kinase P85, p-p38, p-ERK1,2, p-JNK staining the tissues were fixed for 1 h at 4°C in 4% formaldehyde in PBS. Blocking against unspecific binding was performed for 60 min with 10% FCS dissolved in 0.01% PBST. The tissues were subsequently incubated for 90 min at room temperature with primary antibodies dissolved in PBS supplemented with 10% FCS in 0.1% PBST. The tissues were thereafter washed three times with PBST (0.01% Triton) and reincubated with either a Cy5-conjugated goat anti-rat IgG (H+L), a Cy5-conjugated goat anti mouse IgG (H+L), or a Cy5-conjugated goat anti-rabbit IgG (all from Dianova, Hamburg, Germany) at a concentration of 3.8 µg/ml in PBS containing 10% FCS in 0.01% PBST. After washing three times in PBST (0.01% Triton) the tissues were stored in PBS until inspection. Fluorescence recordings were performed by means of a confocal laser scanning setup (Leica TCS SP2, Bensheim, Germany) connected to an inverted microscope (DMIRE2, Leica). The confocal setup was equipped with a 5 mW helium/neon laser, single excitation 633-nm (excitation of Cy5). Emission was recorded at > 665-nm. The pinhole settings of the confocal setup were adjusted to give a full width half maximum (FWHM) of 10 µm. Fluorescence was recorded in a depth of 80 – 120 µm in the depth of the tissue and the fluorescence values in the respective optical section were evaluated by the image analysis software of the confocal setup.

Quantitative RT-PCR - Total RNA from CCE and HM-1 embryoid bodies treated for 24h with the substances as indicated was prepared using Trizol (Invitrogen) method followed by genomic DNA digestion using DNAse I (Invitrogen, Karlsruhe, Germany). Total RNA concentration was determined by OD_{260nm} method. cDNA synthesis was performed using 2µg RNA in a total volume of 20µl with MMLV RT (Invitrogen).Primer concentration for qPCR was 10 pM/20µl. Primer (Invitrogen) sequences were as follows:

HIF-1α: fwd: 5`-TCA CCA GAC AGA GCA GGA AA-3`
rev.: 5`-CTT GAA AAA GGG AGC CAT CA-3`
CTF-1: fwd: 5`-GAACACACAGGACACAGATGGAG -3`
rev.: 5`-GAACACACAGGACACAGATGGAG -3`
NOX1: fwd: 5`-AAT GCC CAG GAT CGA GGT-3`
rev.: 5`-GAT GGA AGC AAA GGG AGT GA-3`
NOX4: fwd: 5`-GAT CAC AGA TCC CTA GCA G-3`
rev.: 5`-GTT GAG GGC ATT CAC CAA GT-3

House keeping genes:
BACT: fwd: 5`-GAT GAC CCA GAT CAT GTT TGA G-3´
rev.: 5`-CCA TCA CAA TGC CTG TGG TA-3`
GAPDH: fwd: 5`- TCG TCC GGT AGA CAA AAT GG-3`
rev.: 5`GAG GTC AAT GAA GGG GTC GT-3`

Amplifications were performed in an Icycler Optical Module (Biorad, Munich, Germany) using iQ^{TM} SYBR Green Supermix (Biorad). Following programmes were used:
Cycle 1: Step 1: 93°C for 15:00 min (1X)
Cycle 2: Step 1: 93°C for 30s (45X)
Step 2: different annealing temperatures for 30s (45X)
Step 3: 72°C for 30s (45X)
Cycle 3: Step 1:50°C for 10 min
Annealing temperatures were
60°C for HIF-1α, Nox-1 and BACT
64°C for CT-1, Nox-4 and GAPDH
HIF-1α and Nox-1 data were normalised against the β –actin (BACT) data and CT-1 and Nox-4 data were normalised against the GAPDH data. The primer concentration was 10 pM/20 µl. Amplifications were performed in an Icycler Optical Module (Biorad) using absolute Sybr Green Fluorescein Mix (Abgene, Absom, UK). Fluorescence increase of SYBR Green was automatically measured after each extension step.
Amplified transcripts were loaded on a 2% Agarose gel. C_T values were automatically obtained. Relative expression values were obtained by normalizing C_T values of the tested genes in comparison with C_T values of the housekeeping genes using the $\Delta\Delta$ C_T Method.

Measurement of ROS generation - Intracellular ROS levels were measured using the fluorescent dye 2´7´-dichlorodihydrofluorescein diacetate (H_2DCF-DA) (Molecular Probes, Eugene, OR), which is a nonpolar compound that is converted into a nonfluorescent polar derivative (H_2DCF) by cellular esterases after incorporation into

cells. H_2DCF is membrane impermeable and is rapidly oxidized to the highly fluorescent 2´,7´-dichlorofluorescein (DCF) in the presence of intracellular ROS. For the experiments, embryoid bodies were incubated in serum-free medium, and 20 µM H_2DCF-DA dissolved in dimethyl sulfoxide (DMSO) was added. After 20 min intracellular DCF fluorescence (corrected for background fluorescence) was evaluated in 3600 µm² regions of interest using an overlay mask unless otherwise indicated. For fluorescence excitation, the 488-nm band of the argon ion laser of the confocal setup was used. Emission was recorded using a longpass LP515-nm filter set.

Statistical analysis - Data are given as mean values ± SD, with *n* denoting the number of experiments unless otherwise indicated. In each experiment 15-20 embryoid bodies were analyzed. Student´s t-test for unpaired data was applied as appropriate. A value of $P < 0.05$ was considered significant.

RESULTS

Time course of CT-1 and gp130 expression during ES cell-derived embryoid body differentiation

Treatment of ES cell-derived embryoid bodies with CT-1 results in stimulation of cardiomyogenesis. Furthermore, CT-1 is endogenously expressed in embryoid bodies (4). To correlate CT-1 expression with the time course of embryoid body differentiation and expression of the transducing receptor gp130, CT-1 and gp130 expression was monitored over the time of cell culture by semiquantitative immunohistochemistry. It was apparent that expression of CT-1 (n = 6) and gp130 (n = 4) followed a comparable kinetics of upregulation until day 8 of cell culture and subsequent downregulation on day 10 and day 11 (Fig. 1*A,B*). The maximum expression of CT-1 and gp130 amounted to 175 ± 25 % and 188 ± 6 %, respectively, on day 8 as compared to day 2 (set to 100 %). It has been previously shown that cardiomyogenic differentiation of mouse ES cells occurs between day 6 and 8, i.e. during the time of maximum CT-1 and gp130 expression (14).

Regulation of CT-1 expression by endogenous generated ROS – correlation with HIF-1α

We have previously shown that differentiating embryoid bodies robustly generate ROS which may be utilized as signalling molecules regulating CT-1 expression (12). To validate this assumption embryoid bodies were treated with the free radical scavenger vitamin E (20 µM) from day 2 to day 8. Subsequently, CT-1 expression was assessed in untreated and vitamin E-treated embryoid bodies. Since CT-1 has been previously shown to be upregulated by hypoxic stress in cardiac myocytes (15) the expression of HIF-1α was assessed in parallel to investigate possible correlation with CT-1 expression. It was apparent that vitamin E treatment downregulated CT-1 as well as HIF-1α expression in 8-day-old embryoid bodies (untreated control set to 100 %), indicating regulation by ROS endogenously generated in differentiating ES cells (Fig. 2) (n = 4).

Regulation of CT-1 and HIF-1α expression by exogenous prooxidants

The experiments of the present study suggest regulation of CT-1 as well as HIF-1α by endogenous generation of ROS during the time course of differentiation. To further validate these findings, embryoid bodies were treated on day 4 of cell culture with either the prooxidants menadione or H_2O_2, and CT-1 as well as HIF-1α protein and mRNA expression was assessed 24 h thereafter (Fig. 3*A,B*). Treatment of embryoid bodies with H_2O_2 in concentrations ranging from 1 nM to 100 µM resulted in dose-dependent increase of CT-1 protein expression (data not shown). Maximum effects were achieved at 10 µM H_2O_2 which increased CT-1 protein (Fig. 3*A*) and mRNA expression (Fig. 3*B*) to 145 ± 8% and 140 ± 9%, respectively (n = 3) (untreated control set to 100 %). Likewise, treatment with 10 µM (data not shown) and 20 µM menadione resulted in increased CT-1 expression with maximum values of 157 ± 8 % and 175 ± 7 % for CT-1 protein (n = 3) (Fig. 3*A*) and mRNA (n = 3) (Fig. 3*B*) expression, respectively, at 20 µM menadione concentration. Under the same experimental conditions increased protein as well as mRNA expression of HIF-1α was observed. HIF-1α protein expression amounted to 140 ± 8% and 184 ± 9% (see Fig. 3*A*), and mRNA expression to 220 ± 24% and 264 ± 7% for H_2O_2 and menadione, respectively (see Fig. 3*B*) (n = 5) thus corroborating the notion of parallel regulation of CT-1 and HIF-1α by prooxidants.

Upregulation of CT-1 and HIF-1α expression by hypoxia

The above experiments suggest that the regulation of CT-1 on the protein as well as mRNA level occurs in parallel to the regulation of HIF-1α. Consequently, it should be assumed that hypoxia, which is well known to upregulate HIF-1α, vice versa results in upregulation of CT-1. To validate this assumption 4-day-old embryoid bodies were treated either for 24 h with physiological (1% O_2) or chemical (50 µM $CoCl_2$) hypoxia and CT-1 as well as HIF-1α protein and mRNA expression were evaluated (Fig. 4*A,B*). According to our working hypothesis physiological (n = 3) as well as chemical hypoxia (n = 4) upregulated CT-1 protein expression to 191 ± 18% and 157 ± 13%, respectively, whereas increased levels of HIF-1α protein amounting to 192 ± 20% (n = 3) and 183 ± 16 % (n = 3) were observed upon physiological and chemical hypoxia, respectively (see Fig. 4*A*). A significant increase in *CT-1* as well as *HIF-1α* mRNA expression amounting to 192 ± 8 % (n = 3) and 279 ± 24 % (n = 4), respectively, was only achieved with chemical hypoxia, whereas only a minor non-significant increase in mRNA expression was observed upon physiological hypoxia (Fig. 4*B*).

Generation of ROS by menadione and chemical hypoxia in embryoid bodies

Since prooxidants as well as chemical hypoxia exerted comparable effects on CT-1 and HIF-1α expression in embryoid bodies it was assumed that both substances utilized the same signalling molecules, i.e. they increased intracellular ROS generation. This was assessed by incubating embryoid bodies with the redox-sensitive fluorescence indicator H_2DCF-DA and determination of DCF fluorescence (Fig. 5*A,B*). When embryoid bodies were treated for 24 h with 20 µM menadione, a significant increase in ROS generation was observed which remained on an elevated niveau even 24 h after replacement of menadione-supplemented cell culture medium with normal medium (Fig. 5*A*) (n = 4). An increase in ROS generation was likewise achieved when embryoid bodies were treated for 24 h with $CoCl_2$ (Fig. 5*B*) (n = 3), suggesting that indeed ROS may act as signalling molecules regulating the expression of CT-1 and HIF-1α following treatment with menadione and chemical hypoxia. This was further corroborated by in experiments where CT-1 expression following treatment with menadione (Fig. 6*A*) (n = 3) and $CoCl_2$ (Fig. 6*B*) (n = 4) was assessed in the presence of the free radical scavengers vitamin E (20 µM) and NMPG (20 µM) which resulted in significant downregulation of CT-1 expression, thus clearly indicating regulation of CT-1 expression by intracellular ROS.

Upregulation of NADPH-oxidase by menadione and hypoxia

Prooxidants may regulate the expression of ROS generating NADPH-oxidase thereby providing a feedforward loop of increased ROS generation even in the absence of external prooxidants. This was evaluated by assessing protein expression of the NADPH-oxidase subunits p22-phox, p47-phox, p67-phox, Nox-1 and Nox-4 as well as mRNA expression of *Nox-1* and *Nox-4* (Fig. 7*A,B*). Preincubation for 24 h with either menadione (20 µM) or $CoCl_2$ (50 µM) significantly increased NADPH oxidase subunit expression on the protein (Fig. 7*A*) (n = 4) as well as mRNA (Fig. 7*B*) level (n = 5) suggesting regulation of CT-1 expression by NADPH-oxidase-derived ROS (n =). Furthermore, treatment with physiological hypoxia (1% O_2) significantly increased protein expression of p22-phox, p47-phox and Nox-4 (data not shown). The involvement of NADPH-oxidase in the regulation of CT-1 expression was further confirmed by incubating embryoid bodies with either menadione (20 µM) or $CoCl_2$ (50 µM) in the presence of the NADPH-oxidase inhibitors DPI (10 µM) (n = 3) or apocynin (10 µM) (n = 3) (Fig. 8). Under these experimental conditions the increase in CT-1 expression following treatment with either menadione or $CoCl_2$ was significantly inhibited, which clearly indicates that NADPH-oxidase-derived ROS are involved in upregulation of CT-1 by prooxidants and hypoxia.

Expression and phosphorylation of gp130 by prooxidants and chemical hypoxia

Regulation of CT-1 expression may be mediated via activation of the gp130 signalling cascade which is initiated through phosphorylation of the gp130 signal transduction receptor. To assess changes in gp130 expression as well as gp130 phosphorylation in the presence of prooxidants and chemical hypoxia semiquantitative immunohistochemistry was performed using antibodies against the unphosphorylated as well as the phosphorylated form of gp130. It was found that prooxidants as well as chemical hypoxia significantly increased gp130 expression as well as phosphorylation, suggesting activation of gp130-mediated signal transduction cascades (n = 3) (Fig. 9).

Signalling cascades involved in the upregulation of CT-1 by menadione and chemical hypoxia

Upon binding of CT-1 to a heterodimer of LIFR-ß and gp130 a complex signalling cascade is activated which involves the MAPK members ERK1,2, JNK and p38 as well as PI3-kinase and the Jak/STAT pathway. Since the data of the present study demonstrated phosphorylation of gp130 it was investigated whether downstream MAPK and PI3-kinase signalling cascades were activated by treatment of embryoid bodies with menadione and chemical hypoxia (Fig. 10). By using phospho-specific antibodies it was found that phosphorylation of ERK1,2 (maximum after 15 min) (menadione, n = 3; $CoCl_2$, n = 5), JNK (maximum after 15 min, menadione treatment; maximum after 30 min, $CoCl_2$ treatment) (menadione, n = 3; $CoCl_2$, n = 5), p38 (maximum after 30 min, menadione treatment; maximum after 60 min, $CoCl_2$ treatment) (menadione, n = 4; $CoCl_2$, n = 4), and PI3-kinase (maximum after 60 min) (n = 4) occurred. To correlate the activation of MAPK pathways and PI3-kinase to the expression of CT-1, embryoid bodies were treated with the ERK1,2 inhibitor UO126 (10 µM), the JNK inhibitor SP600125 (10 µM) the p38 inhibitor SKF86002 (10 µM) as well as the PI3-kinase inhibitor LY294002 (20 µM) which significantly downregulated the menadione- and $CoCl_2$-induced upregulation of CT-1 (n = 3) (Fig. 11). A comparable inhibition of CT-1 expression was achieved when the Jak/STAT signalling pathway was inhibited with the Jak-2 antagonist AG490 (data not shown).

Absence of cardiomyogenesis and stimulation of CT-1 expression in HIF-1$\alpha^{-/-}$ ES cells

The data of the present study suggest that menadione and hypoxia stimulate CT-1 expression in embryoid bodies by a mechanism regulated through the transcription factor HIF-1α. To prove this working hypothesis to be true, embryoid bodies grown from the CCE cell line were treated with the HIF-1α inhibitor 2-ME (3 µM) and upregulation of CT-1 protein expression upon menadione treatment and chemical hypoxia was assessed (Fig. 12). Furthermore, HM-1 HIF-1$\alpha^{-/-}$ ES cells were employed in the experiments (Fig. 13*A*-*C*). Treatment with 2-ME totally abolished the increase in HIF-1α expression observed after menadione (20 µM) treatment (n = 5), data not shown. In corroboration of our working hypothesis it was apparent that in the presence of 2-ME menadione- and chemical hypoxia-induced upregulation of CT-1 was significantly attenuated (see Fig. 12) (n = 5). In HIF-1$\alpha^{-/-}$ ES cells cardiomyogenesis was completely absent as compared to the wild-type control (see Fig. 13*A*), and no upregulation of CT-1 during the time course of differentiation as compared to wt HM-1 ES cells (see Fig. 13*B*) and ES cells of the CCE cell line (see Fig. 1*A*) was observed (n = 5). Furthermore, the upregulation of CT-1 mRNA expression following treatment of embryoid bodies with menadione and $CoCl_2$ was completely abolished (see Fig. 13*C*) (n = 6) which clearly indicates regulation of CT-1 expression by HIF-1α.

DISCUSSION

The present study reports on the regulation of CT-1 expression by HIF-1α via signaling cascades involving ROS. Hypoxia is a common situation occurring during conditions where increased expression of CT-1 has been reported: (*a*) during cardiac diseases like angina pectoris, cardiac infarction and heart failure (7); (*b*) in the embryonic heart where the heart mass increases through cardiac cell hyperplasia (16); (*c*) during the growth of ES cells within the 3-dimensional tissue of embryoid bodies (17). Recently, it has been demonstrated that hypoxia is associated with increased ROS generation produced either through the mitochondrial respiratory chain or NADPH-oxidase activity (18). ROS are well known to act as signaling molecules in a variety of growth factor and cytokine-mediated signaling pathways that include CT-1 (19). Furthermore, elevated ROS are known to occur in cardiac infarction and are suspected to cause ischemia-reperfusion injury (20). Last but not least low level ROS have been shown to stimulate ES cell-derived cardiomyocyte differentiation as well as proliferation (12;21).

Although hypoxia has been previously demonstrated to induce CT-1 expression (15), the underlying signaling cascades have not been elucidated nor has any connection between hypoxia, ROS generation and CT-1 expression been established. In ES cells differentiating within embryoid bodies occurrence of hypoxia (17) and endogenous generation of ROS via NADPH-oxidase (12;21) has been previously evidenced, which led to the working hypothesis of the present study that hypoxia and ROS may regulate CT-1 expression. This assumption was corroborated by the data of the present study

demonstrating that incubation of ES cell-derived embryoid bodies with free radical scavengers downregulated CT-1 and HIF-1α expression. Vice versa our experiments showed that prooxidants as well as physiological and chemical hypoxia upregulated CT-1 as well as HIF-1α protein and mRNA expression. Furthermore, either menadione treatment or chemical hypoxia resulted in increased ROS generation with subsequent upregulation of ROS-generating NADPH-oxidase which strongly suggests that under conditions of prooxidant incubation and hypoxia the same ROS-mediated signaling pathways are utilized.

Elevated ROS levels during hypoxia have been previously shown to occur in pulmonary myocytes (22), cardiac myocytes, Hep3B cells, HeLa cells (23) as well as adipocytes (24), the sources being either the mitochondrial respiratory chain or NADPH-oxidase. These ROS may regulate the so far scarcely defined non-hypoxic pathway of HIF-1α stabilization, translocation and activation (25;26). On the basis of the properties of Nox oxidases it has been recently proposed that hypoxia could cause an acute increase in ROS production by augmenting rates of electron transport to cytochrome b_{558}, and this could occur through hypoxia-promoting oxidase activation and/or increasing the availability of its NADH or NADPH substrates (18). The data of the present study clearly point towards a distinct role of NADPH-oxidase-derived ROS in the regulation of CT-1 expression in ES cells since inhibition of NADPH-oxidase by apocyin as well as DPI abolished prooxidant and chemical hypoxia-mediated induction of CT-1. The involvement of ROS in the regulation of CT-1 expression was further validated by experiments demonstrating that the effects observed with the prooxidant menadione and chemical hypoxia were significantly inhibited in the presence of free radical scavengers.

The regulation of cytokine expression by HIF-1α and ROS has been recently discussed (25). Expression of cytokines is generally associated to states of hypoxia, ROS generation and inflammation, i.e. pathophysiologic situations that require an immunological response as well as protection from tissue injury. Previously, stimulation of mRNA expression as well as secretion of IL-6 in response to exposure with prooxidants has been shown (27-29) and may act in paracrine as well as autocrine manner, thereby activating a loop mechanism disposed to stimulate the cell´s IL-6 receptors. This autocrine loop of cytokine activation and secretion may be initiated by prooxidants acting on the IL-6 signaling cascade. In this respect, the data of the current study demonstrated stimulation of gp130 protein expression as well as phosphorylation by prooxidants and chemical hypoxia, and downstream activation of several members of the previously described (30), CT-1 activated signal transduction cascade, i.e. the MAPKs ERK1,2, JNK, p38 as well as PI3-kinase which indeed suggests activation of the CT-1-mediated signaling cascade by ROS. Consequently, the data of the present study demonstrated that inhibition of all investigated MAPK pathways, PI3-kinase as well as the Jak/STAT pathway, abolished the prooxidant- and hypoxia-mediated increase in CT-1 and HIF-1α expression.

The transcription factor HIF-1α binds to hypoxia-responsive elements (HRE) in the enhancers of several hypoxia-regulated genes including VEGF and erythropoietin. The mouse *CT-1* gene has been recently isolated (31). It constitutes 5.4 kilobases (kb) in length and consists of three exons and two introns. When nucleotide sequences of the coding regions of exons were compared with those of human, it was observed that exon 1, 2 and 3 share 96%, 84% and 81% homology, respectively. Interestingly, potential binding sites for several ubiquitous transcription factors including HIF-1α were present in the 5´-flanking region extending 2174-bp upstream from the transcription initiation site (31) which underscores the notion of the present study of *CT-1* regulation by signal transduction pathways that involve HIF-1α.

If CT-1 expression is indeed regulated by HIF-1α, absence of hypoxia- and prooxidant-mediated upregulation of CT-1 should be anticipated under conditions of either pharmacological or genetic inactivation of HIF-1α. This was investigated by either a pharmacological approach using 2-ME which has been recently shown to downregulate HIF-1α at the posttranscriptional level and inhibits HIF-1-induced transcriptional activation of VEGF expression (32) or by ES cells homozygous deficient for HIF-1α (13). Although basal mRNA and protein expression of CT-1 was found in HIF-1$\alpha^{-/-}$ cells (data not shown), upregulation during the time course of ES cell differentiation as occurring in wt cells was not observed, and cardiomyogenesis was completely absent. Furthermore, prooxidants as well as chemical hypoxia failed to upregulate CT-1 in

HIF-1α$^{-/-}$ ES cells which clearly demonstrates regulation of CT-1 expression by HIF-1α.

Although the classical view of HIF-1 regulation proposed stabilization of HIF-1α under hypoxic conditions and downregulation at normoxia by process of pVHL-mediated ubiquitin-proteasome pathway, mechanisms of HIF-1α stabilization under normoxic conditions have been recently proposed (33). These non-hypoxic pathways are utilized by many growth factors and cytokines, including insulin-like growth factors (34), transforming growth factor and platelet-derived growth factor (35), and IL-1ß (36) which are all known to utilize ROS as signaling molecules within their signal transduction cascade. In this regard it was demonstrated that inhibition of ROS generation abolished hormone and growth factor-mediated increase in HIF-1α (37). The data of the presents study demonstrate ROS generation under conditions of either chemical or physiological hypoxia which was recently also reported to occur in intrapulmonary arteries of mice (38), in skeletal muscle (39) and in human hepatoma cells (40). This was underscored by the observation that oxygen sensing during hypoxia is dependent on mitochondrial-generated ROS (41;42).

Regulation of CT-1 expression by HIF-1α and ROS sounds reasoning in light of its biological function in inhibiting cardiac cell apoptosis, promoting cardiac cell hypertrophy and stimulating embryonic cardiac cell differentiation and proliferation which are phenomena occurring under conditions of hypoxia and/or ROS-mediated inflammation. The role of ROS in hypoxic/non-hypoxic pathways of HIF-1α regulation require further research efforts. The investigation of the physiological microenvironment that regulates CT-1 expression will not only assist to unravel the role of CT-1 in cardiac hypertrophy and cardiac repair in the infarcted heart, but also give clues to the understanding of the mechanisms of cardiac cell hyperplasia in the embryonic heart and cardiomyogenic differentiation of ES cells.

FOOT NOTES

This grant was supported by the German Research Foundation (DFG) grant SA884/4-1.

REFERENCES

1. Freed, D. H., Cunnington, R. H., Dangerfield, A. L., Sutton, J. S., and Dixon, I. M. (2005) *Cardiovasc.Res.* **65,** 782-792

2. Pennica, D., Wood, W. I., and Chien, K. R. (1996) *Cytokine Growth Factor Rev.* **7,** 81-91

3. Sheng, Z., Pennica, D., Wood, W. I., and Chien, K. R. (1996) *Development* **122,** 419-428

4. Sauer, H., Neukirchen, W., Rahimi, G., Grunheck, F., Hescheler, J., and Wartenberg, M. (2004) *Exp.Cell Res.* **294,** 313-324

5. Wollert, K. C., Taga, T., Saito, M., Narazaki, M., Kishimoto, T., Glembotski, C. C., Vernallis, A. B., Heath, J. K., Pennica, D., Wood, W. I., and Chien, K. R. (1996) *J.Biol.Chem.* **271,** 9535-9545

6. Sheng, Z., Knowlton, K., Chen, J., Hoshijima, M., Brown, J. H., and Chien, K. R. (1997) *J.Biol.Chem.* **272,** 5783-5791

7. Freed, D. H., Moon, M. C., Borowiec, A. M., Jones, S. C., Zahradka, P., and Dixon, I. M. (2003) *Mol.Cell Biochem.* **254,** 247-256

8. Brar, B. K., Stephanou, A., Liao, Z., O'Leary, R. M., Pennica, D., Yellon, D. M., and Latchman, D. S. (2001) *Cardiovasc.Res.* **51,** 265-274

9. Liao, Z., Brar, B. K., Cai, Q., Stephanou, A., O'Leary, R. M., Pennica, D., Yellon, D. M., and Latchman, D. S. (2002) *Cardiovasc.Res.* **53,** 902-910

10. Talwar, S., Squire, I. B., Downie, P. F., Davies, J. E., and Ng, L. L. (2000) *Heart* **84,** 421-424

11. Talwar, S., Squire, I. B., Downie, P. F., O'Brien, R. J., Davies, J. E., and Ng, L. L. (2000) *Clin.Sci.(Lond)* **99,** 83-88

12. Sauer, H., Rahimi, G., Hescheler, J., and Wartenberg, M. (2000) *FEBS Lett.* **476,** 218-223

13. Hopfl, G., Wenger, R. H., Ziegler, U., Stallmach, T., Gardelle, O., Achermann, R., Wergin, M., Kaser-Hotz, B., Saunders, H. M., Williams, K. J., Stratford, I. J., Gassmann, M., and Desbaillets, I. (2002) *Cancer Res.* **62,** 2962-2970

14. Hescheler, J., Wartenberg, M., Fleischmann, B. K., Banach, K., Acker, H., and Sauer, H. (2002) *Methods Mol.Biol.* **185,** 169-187

15. Hishinuma, S., Funamoto, M., Fujio, Y., Kunisada, K., and Yamauchi-Takihara, K. (1999) *Biochem.Biophys.Res.Commun.* **264,** 436-440

16. Wikenheiser, J., Doughman, Y. Q., Fisher, S. A., and Watanabe, M. (2005) *Dev.Dyn.*

17. Wartenberg, M., Donmez, F., Ling, F. C., Acker, H., Hescheler, J., and Sauer, H. (2001) *FASEB J.* **15,** 995-1005

18. Wolin, M. S., Ahmad, M., and Gupte, S. A. (2005) *Am.J.Physiol Lung Cell Mol.Physiol* **289,** L159-L173

19. Sauer, H., Wartenberg, M., and Hescheler, J. (2001) *Cell Physiol Biochem.* **11,** 173-186

20. Berg, K., Jynge, P., Bjerve, K., Skarra, S., Basu, S., and Wiseth, R. (2005) *Free Radic.Res.* **39,** 629-636

21. Sauer, H., Rahimi, G., Hescheler, J., and Wartenberg, M. (1999) *J.Cell Biochem.* **75,** 710-723

22. Marshall, C., Mamary, A. J., Verhoeven, A. J., and Marshall, B. E. (1996) *Am.J.Respir.Cell Mol.Biol.* **15,** 633-644

23. Chandel, N. S., Maltepe, E., Goldwasser, E., Mathieu, C. E., Simon, M. C., and Schumacker, P. T. (1998) *Proc.Natl.Acad.Sci.U.S.A* **95,** 11715-11720

24. Carriere, A., Fernandez, Y., Rigoulet, M., Penicaud, L., and Casteilla, L. (2003) *FEBS Lett.* **550,** 163-167

25. Haddad, J. J. and Harb, H. L. (2005) *Int.Immunopharmacol.* **5,** 461-483

26. Haddad, J. J. (2002) *Cell Signal.* **14,** 879-897

27. Kosmidou, I., Vassilakopoulos, T., Xagorari, A., Zakynthinos, S., Papapetropoulos, A., and Roussos, C. (2002) *Am.J.Respir.Cell Mol.Biol.* **26,** 587-593

28. Kida, H., Yoshida, M., Hoshino, S., Inoue, K., Yano, Y., Yanagita, M., Kumagai, T., Osaki, T., Tachibana, I., Saeki, Y., and Kawase, I. (2005) *Am.J.Physiol Lung Cell Mol.Physiol* **288,** L342-L349

29. Haddad, J. J. (2002) *Biochem.Biophys.Res.Commun.* **296,** 847-856

30. Heinrich, P. C., Behrmann, I., Haan, S., Hermanns, H. M., Muller-Newen, G., and Schaper, F. (2003) *Biochem.J.* **374,** 1-20

31. Funamoto, M., Hishinuma, S., Fujio, Y., Matsuda, Y., Kunisada, K., Oh, H., Negoro, S., Tone, E., Kishimoto, T., and Yamauchi-Takihara, K. (2000) *J.Mol.Cell Cardiol.* **32,** 1275-1284

32. Mabjeesh, N. J., Escuin, D., LaVallee, T. M., Pribluda, V. S., Swartz, G. M., Johnson, M. S., Willard, M. T., Zhong, H., Simons, J. W., and Giannakakou, P. (2003) *Cancer Cell* **3,** 363-375

33. Lee, J. W., Bae, S. H., Jeong, J. W., Kim, S. H., and Kim, K. W. (2004) *Exp.Mol.Med.* **36,** 1-12

34. Feldser, D., Agani, F., Iyer, N. V., Pak, B., Ferreira, G., and Semenza, G. L. (1999) *Cancer Res.* **59,** 3915-3918

35. Gorlach, A., Diebold, I., Schini-Kerth, V. B., Berchner-Pfannschmidt, U., Roth, U., Brandes, R. P., Kietzmann, T., and Busse, R. (2001) *Circ.Res.* **89,** 47-54

36. Hellwig-Burgel, T., Rutkowski, K., Metzen, E., Fandrey, J., and Jelkmann, W. (1999) *Blood* **94,** 1561-1567

37. Richard, D. E., Berra, E., and Pouyssegur, J. (2000) *J.Biol.Chem.* **275,** 26765-26771

38. Liu, J. Q., Zelko, I. N., Erbynn, E. M., Sham, J. S., and Folz, R. J. (2005) *Am.J.Physiol Lung Cell Mol.Physiol*

39. Zuo, L. and Clanton, T. L. (2005) *Am.J.Physiol Cell Physiol* **289,** C207-C216

40. Chandel, N. S., McClintock, D. S., Feliciano, C. E., Wood, T. M., Melendez, J. A., Rodriguez, A. M., and Schumacker, P. T. (2000) *J.Biol.Chem.* **275,** 25130-25138

41. Brunelle, J. K., Bell, E. L., Quesada, N. M., Vercauteren, K., Tiranti, V., Zeviani, M., Scarpulla, R. C., and Chandel, N. S. (2005) *Cell Metab* **1,** 409-414

42. Emerling, B. M., Platanias, L. C., Black, E., Nebreda, A. R., Davis, R. J., and Chandel, N. S. (2005) *Mol.Cell Biol.* **25,** 4853-4862

FIGURE LEGENDS

Fig.1. Protein expression of CT-1 (*A*) and gp130 (*B*) during the time course of differentiation of ES cells within the three-dimensional tissue of embryoid bodies. Note, that cardiac cell differentiation occurs during day 6 and 8 of embryoid body cell culture (14).

Fig.2. Regulation of CT-1 and HIF-1α expression in embryoid bodies by endogenous ROS. Embryoid bodies were incubated from day 2 to day 8 of cell culture with 20 µM vitamin E. On day 8 protein expression of CT-1 and HIF-1α was assessed by semiquantitative immunohistochemistry in whole mount embryoid bodies. The images show representative embryoid bodies labelled with antibodies either against CT-1 (*a*,*b*) or HIF-1α (*c*,*d*) which remained untreated (*a*,*c*) or were treated with vitamin E. The bar represents 200 µm. *$P < 0.05$, significantly different to the untreated control.

Fig.3. Upregulation of CT-1 and HIF-1α protein (*A*) and mRNA (*B*) upon treatment with the prooxidants menadione (20 µM) and H_2O_2 (10 µM). Embryoid bodies were treated on day 4 of cell culture with the respective substances and were examined 24 h thereafter. The images show representative embryoid bodies labelled with antibodies against CT-1 (left panel) and HIF-1α (right panel) which remained either untreated (*a*,*d*) or were treated with menadione (*b*,*e*) or H_2O_2 (*c*,*f*). The bar represents 200 µm. *$P < 0.05$, significantly different to the untreated control.

Fig.4. Upregulation of CT-1 and HIF-1α protein (*A*) and mRNA (*B*) upon treatment with the prooxidants menadione and H_2O_2. Embryoid bodies were treated on day 4 of cell culture with either physiological (1% O_2) or chemical ($CoCl_2$) hypoxia and were examined 24 h thereafter. The images show representative embryoid bodies labelled with antibodies against CT-1 (left panel) and HIF-1α (right panel) which remained either untreated (*a*,*d*) or were treated with 1% O_2 (*b*,*e*) or $CoCl_2$ (50 µM) (*c*,*f*). The bar represents 200 µm.*$P < 0.05$, significantly different to the untreated control.

Fig. 5. Generation of ROS following treatment with menadione (A) or under conditions of chemical hypoxia ($CoCl_2$ treatment) (*B*). In *A*, embryoid bodies were treated for 24 h with 20 µM menadione. Subsequently, the cell culture medium was exchanged with medium devoid of menadione, and ROS were monitored at different times after removal of menadione. *B*, ROS generation in the presence of either menadione (20 µM) or $CoCl_2$ (50 µM). *$P < 0.05$, significantly different to the untreated control.

Fig. 6. Inhibition of menadione- (*A*) and $CoCl_2$-mediated (*B*) upregulation of CT-1 upon preincubation with either the free radical scavenger vitamin E (20 µM) or NMPG (20 µM). Embryoid bodies were treated at day 4 of cell culture with either menadione (20 µM) or $CoCl_2$ (50 µM) in the presence of free radical scavengers. Following 24 h CT-1 protein expression was determined by semiquantitative immunohistochemistry. *$P < 0.05$, significantly different as indicated.

Fig. 7. Upregulation of NADPH-oxidase subunits upon incubation of embryoid bodies with menadione and $CoCl_2$. *A*, increase in protein expression of the NADPH-oxidase subunits p22-phox, p47-phox, p69-phox, Nox-1 and Nox-4 which were determined 24 h after treatment of 4-day-old embryoid bodies by semiquantitative immunohistochemistry. *B*, mRNA expression of *Nox-1* and *Nox-4* upon either menadione (20 µM) or $CoCl_2$ (50 µM) treatment. *$P < 0.05$, significantly different to the untreated control.

Fig. 8. Inhibition of menadione- and $CoCl_2$-mediated upregulation of CT-1 upon preincubation with the NADPH-oxidase inhibitors DPI (10 µM) or apocynin (10 µM). Embryoid bodies were treated at day 4 of cell culture with either menadione (20 µM) or $CoCl_2$ (50 µM) in the presence of either DPI or apocynin. Following 24 h CT-1 protein expression was determined by semiquantitative immunohistochemistry. The image show representative embryoid bodies: *a*, untreated; *b*, menadione-treated; *c*, $CoCl_2$-treated; *d*, DPI-treated; *e*, DPI- + menadione-treated; *f*, DPI- + $CoCl_2$-treated; *g*, apocynin-treated; *h*, apocynin- + menadione-treated; *i*, apocynin- + $CoCl_2$-treated. The bar represents 400 µm. *$P < 0.05$, significantly different as indicated.

Fig. 9. Upregulation of gp130 protein expression and phosphorylation upon treatment of embryoid bodies with prooxidants or chemical hypoxia. Embryoid bodies were treated at day 4 of cell culture with either H_2O_2 (10 µM), menadione (20 µM) or $CoCl_2$ (50 µM). After 24 h gp130 protein expression and phosphorylation was assessed by quantitative immunohistochemistry using an antibody directed against unphosphorylated gp130 or the phosphorylated form of gp130. *P < 0.05, significantly different to the untreated control.

Fig.10. Activation of ERK1,2, JNK p38 and PI3-kinase upon incubation of embryoid bodies with either menadione (20 µM) or $CoCl_2$ (50 µM). Activation was assessed by semiquantitative immunohistochemistry using phospho-specific antibodies. Maximum activation of ERK1,2 was achieved after 15 min; maximum activation of JNK was at 15 min for menadione treatment and 30 min for $CoCl_2$ treatment; maximum activation of p38 was at 30 min for menadione treatment and 60 min for $CoCl_2$ treatment; maximum activation of PI3-kinase was at 60 min. *P < 0.05, significantly different to the untreated control.

Fig. 11. Inhibition of menadione- and $CoCl_2$-mediated upregulation of CT-1 by the ERK1,2 inhibitor UO126 (10 µM), the JNK inhibitor SP600125 (10 µM), the p38 inhibitor SKF86002 (10 µM), and the PI3-kinase inhibitor LY294002 (20 µM). Embryoid bodies were treated at day 4 of cell culture with either menadione (20 µM) or $CoCl_2$ in the presence of the respective inhibitor. CT-1 protein expression was assessed following 24 h by semiquantitative immunohistochemistry. *P < 0.05, significantly different as indicated.

Fig. 12. Inhibition of menadione- and $CoCl_2$-mediated upregulation of CT-1 by the HIF-1α inhibitor 2-ME (3 µM). Embryoid bodies were treated at day 4 of cell culture with either menadione (20 µM) or $CoCl_2$ in the presence of 2-ME. CT-1 protein expression was assessed following 24 h by semiquantitative immunohistochemistry. *P < 0.05, significantly different as indicated.

Fig. 13. Cardiac cell differentiation in wt and HIF-1$\alpha^{-/-}$ ES cells (*A*), expression of CT-1 during the time of differentiation (*B*) and upon incubation with menadione (20 µM) and $CoCl_2$ (50 µM) (*C*). In HIF-1$\alpha^{-/-}$ ES cells cardiomyogenesis was completely absent as evaluated by counting the number of spontaneously contracting embryoid bodies (see, *A*). Furthermore, no upregulation of CT-1 mRNA was observed in HIF-1$\alpha^{-/-}$ as compared to the wt (see, *B*). Menadione as well as $CoCl_2$ failed to upregulate CT-1 mRNA in HIF-1$\alpha^{-/-}$ cells. *P < 0.05, significantly different to wt embryoid bodies.

Figure 1

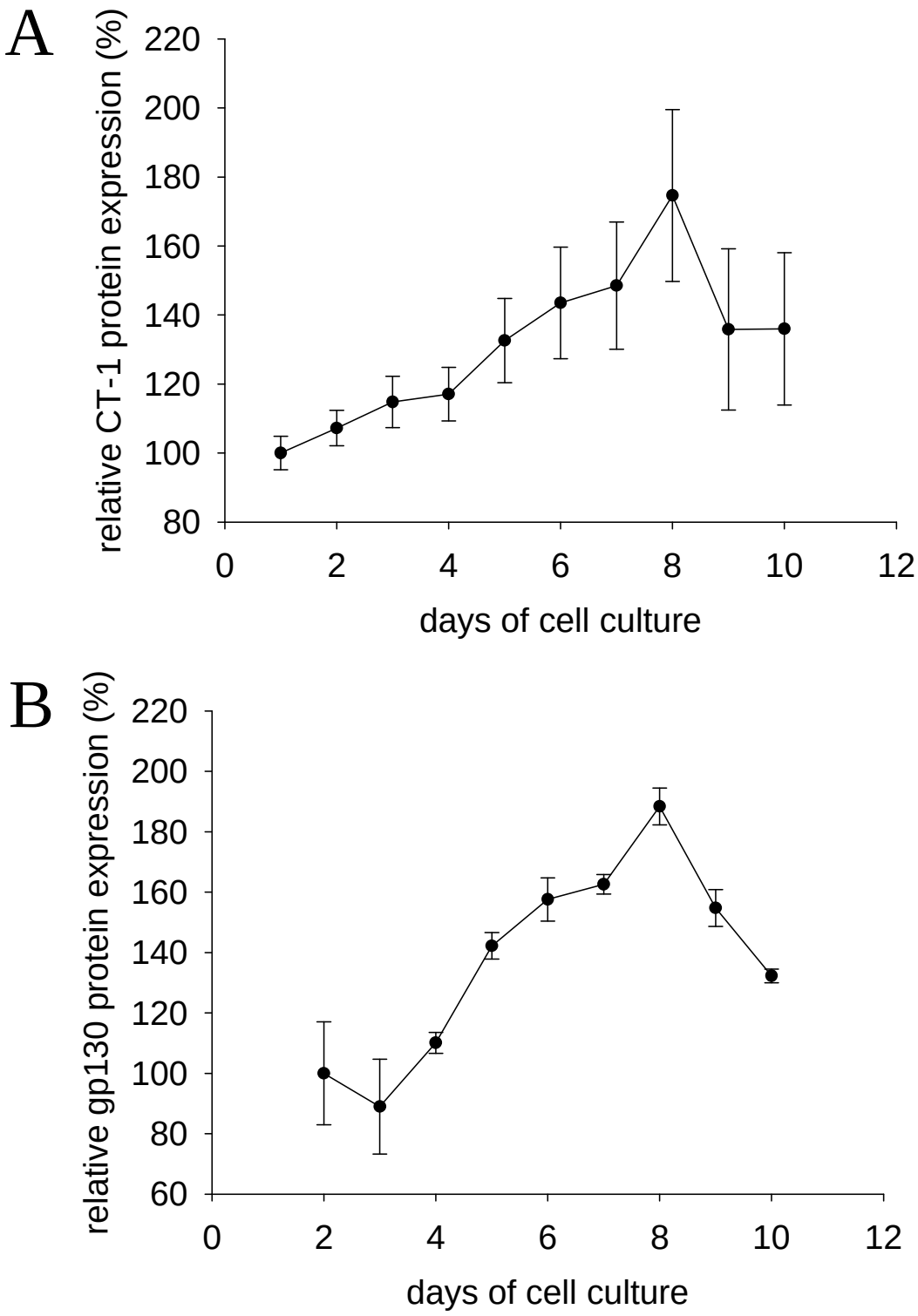
A
relative CT-1 protein expression (%)
220
200
180
160
140
120
100
80
0
2
4
6
8
10
12
days of cell culture
B
relative gp130 protein expression (%)
220
200
180
160
140
120
100
80
60
0
2
4
6
8
10
12
days of cell culture

Figure 2

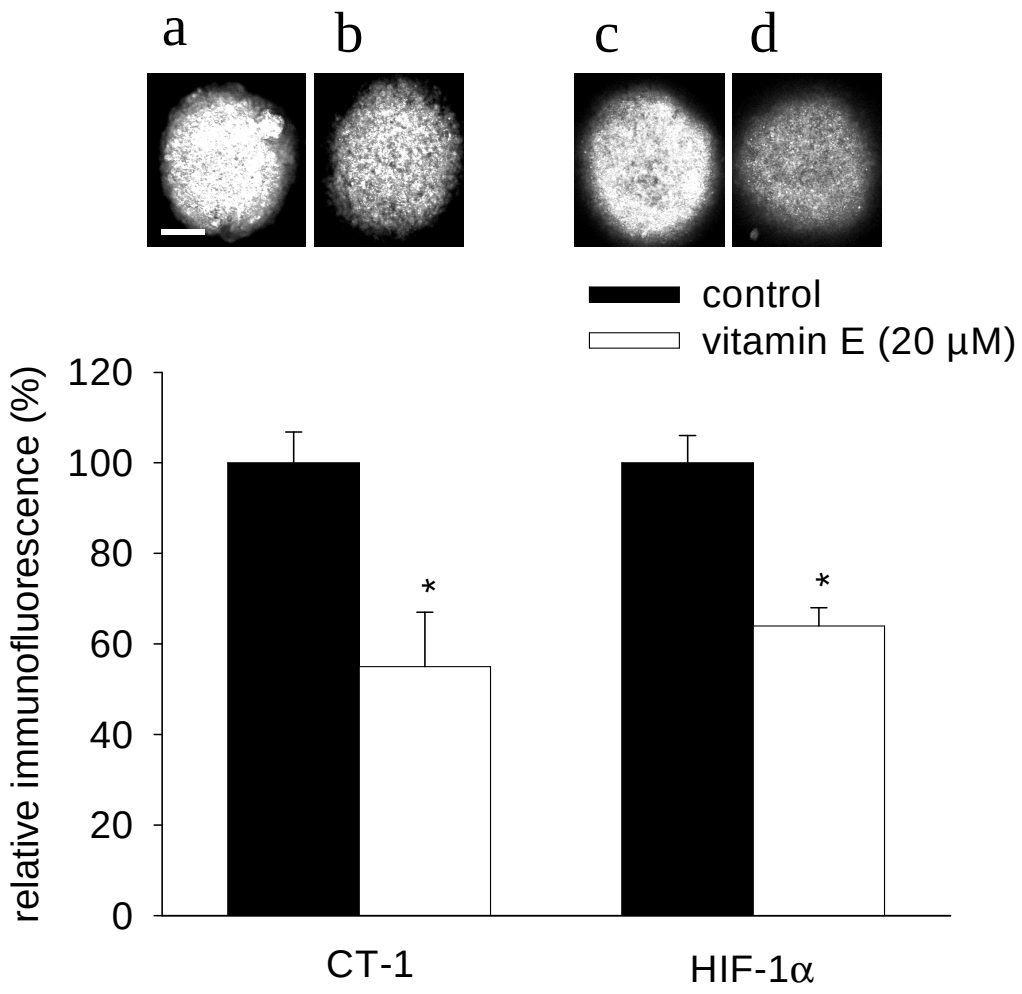
a
b
c
d
control
vitamin E (20 µM)
relative immunofluorescence (%)
120
100
80
60
40
20
0
*
*
CT-1
HIF-1α

Figure 3

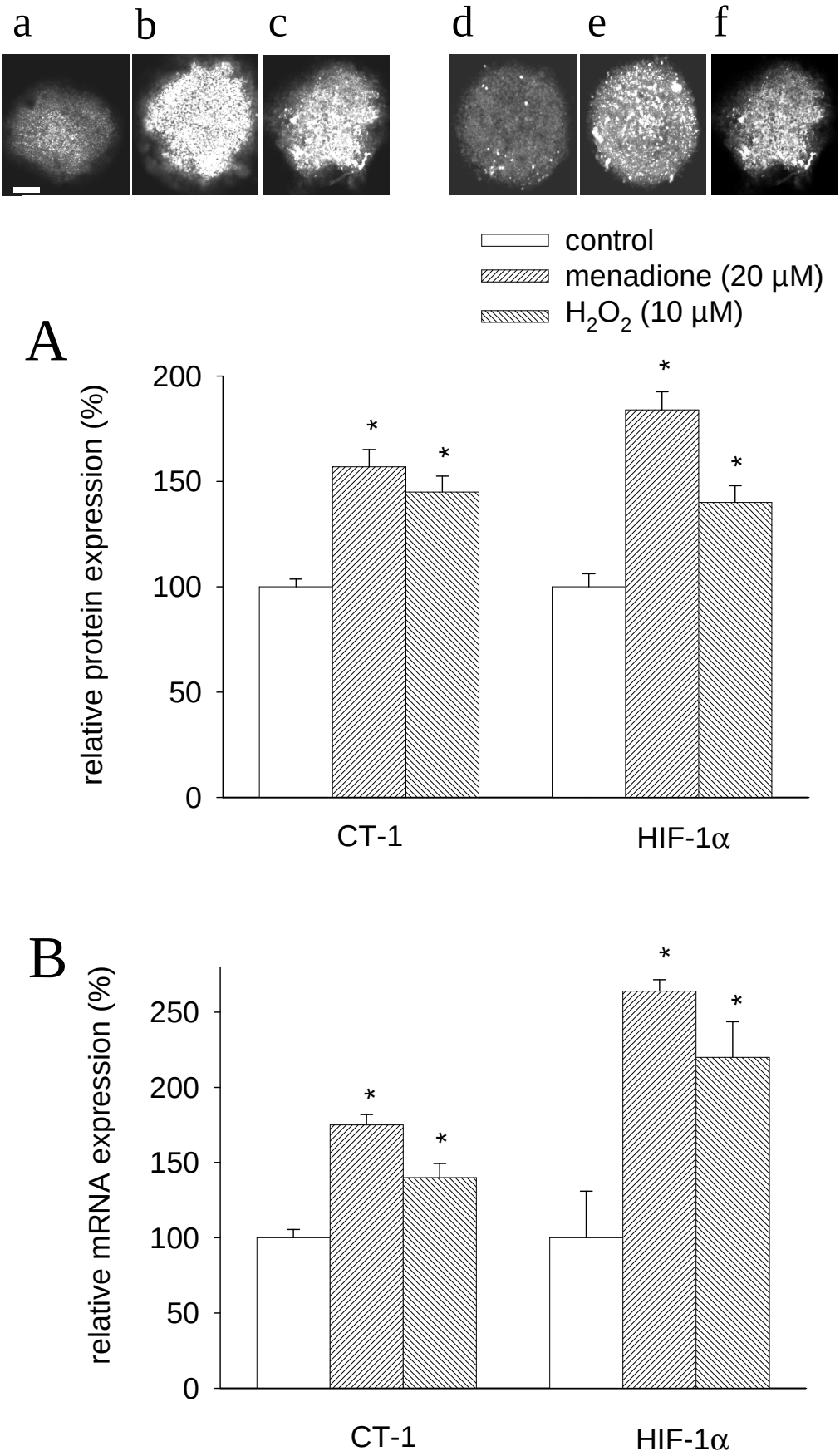
a
b
c
d
e
f
control
menadione (20 µM)
H2O2 (10 µM)
A
relative protein expression (%)
200
150
100
50
0
*
CT-1
HIF-1α
B
relative mRNA expression (%)
250
200
150
100
50
0
CT-1
HIF-1α

Figure 4

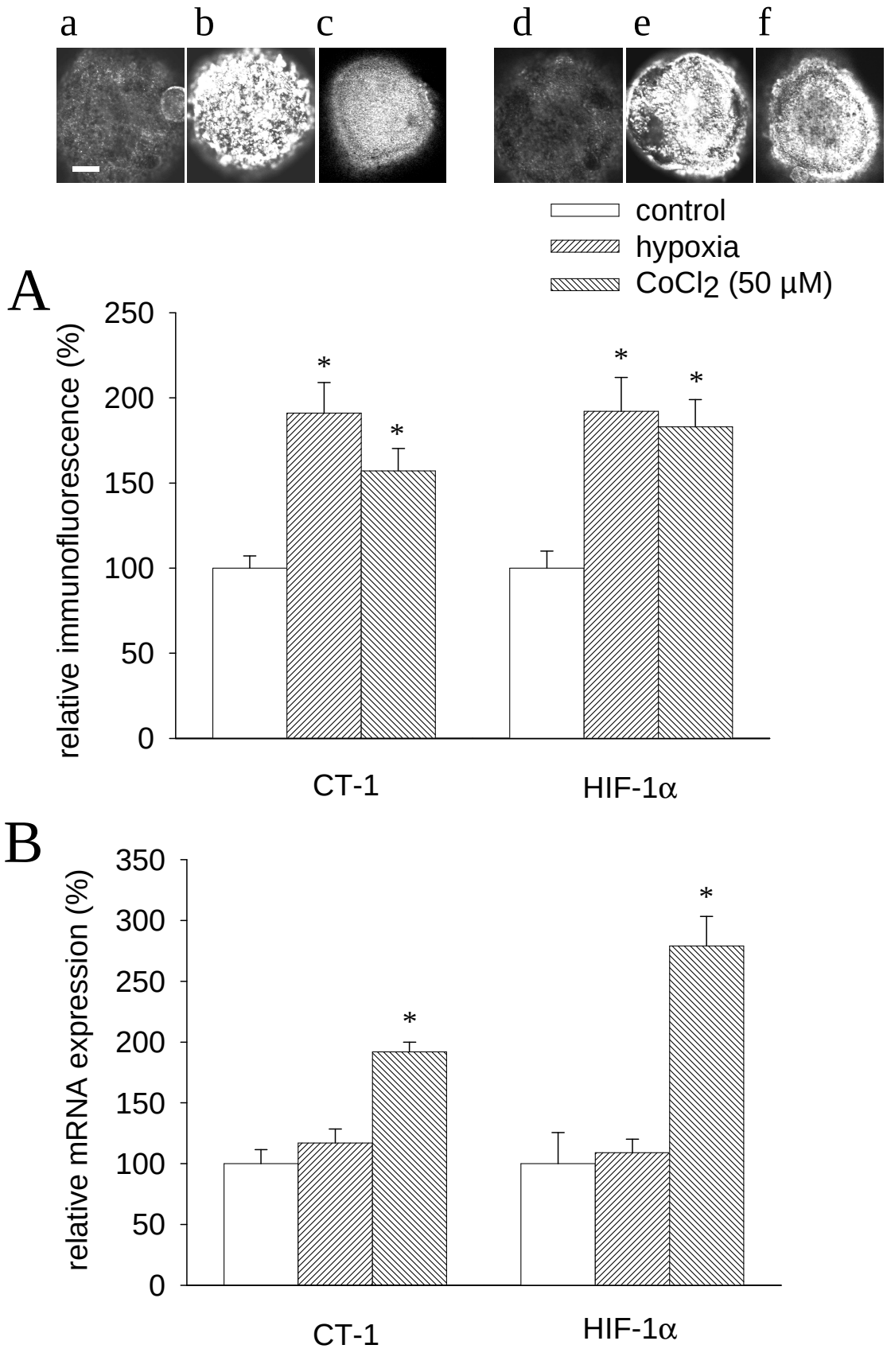
a
b
c
d
e
f
control
hypoxia
CoCl2 (50 µM)
A
relative immunofluorescence (%)
250
200
150
100
50
0
*
*
*
*
CT-1
HIF-1α
B
relative mRNA expression (%)
350
300
250
200
150
100
50
0
*
*
CT-1
HIF-1α

Figure 5

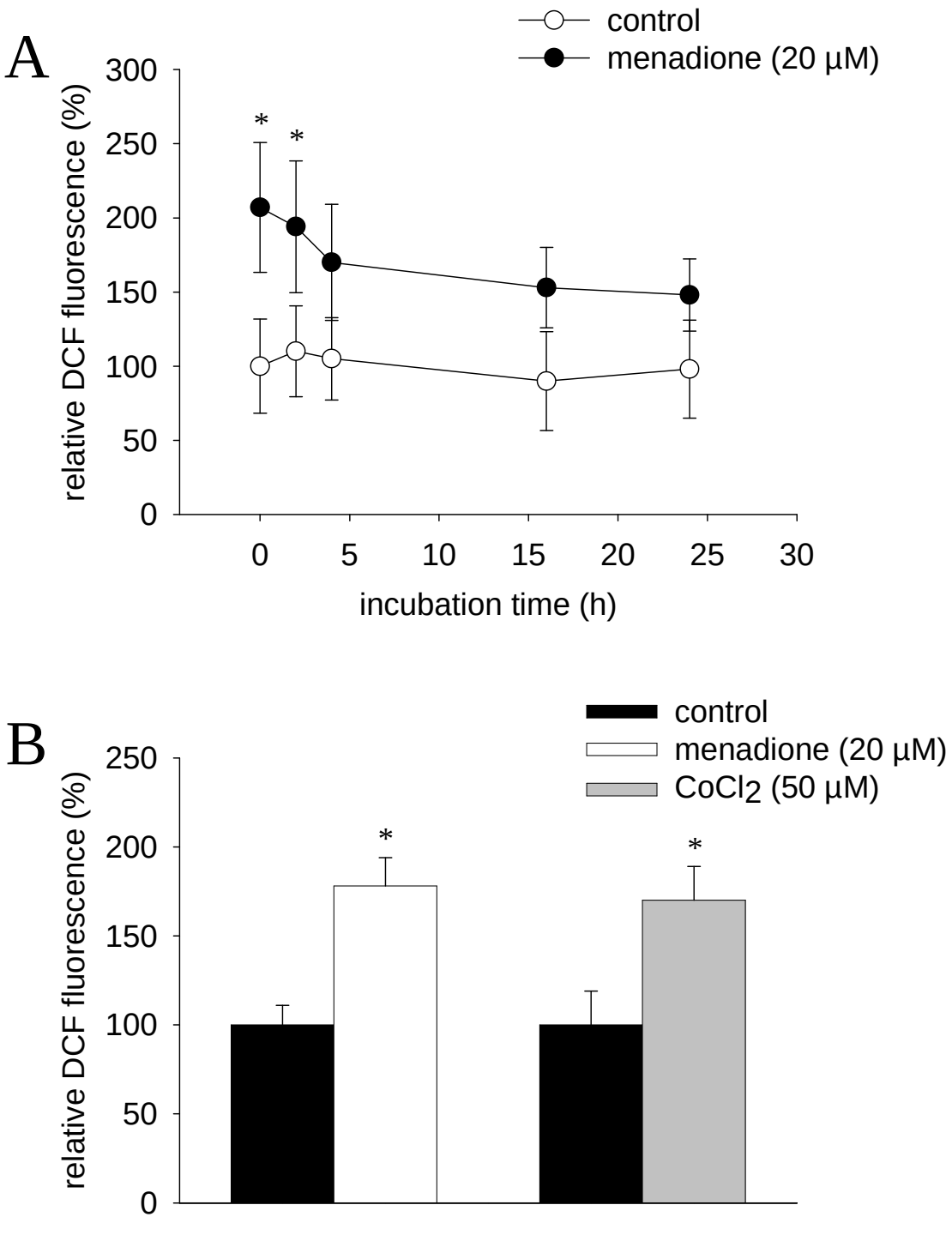
A
control
menadione (20 µM)
relative DCF fluorescence (%)
300
250
200
150
100
50
0
*
*
0
5
10
15
20
25
30
incubation time (h)
B
control
menadione (20 µM)
CoCl2 (50 µM)
relative DCF fluorescence (%)
250
200
150
100
50
0
*
*

Figure 6

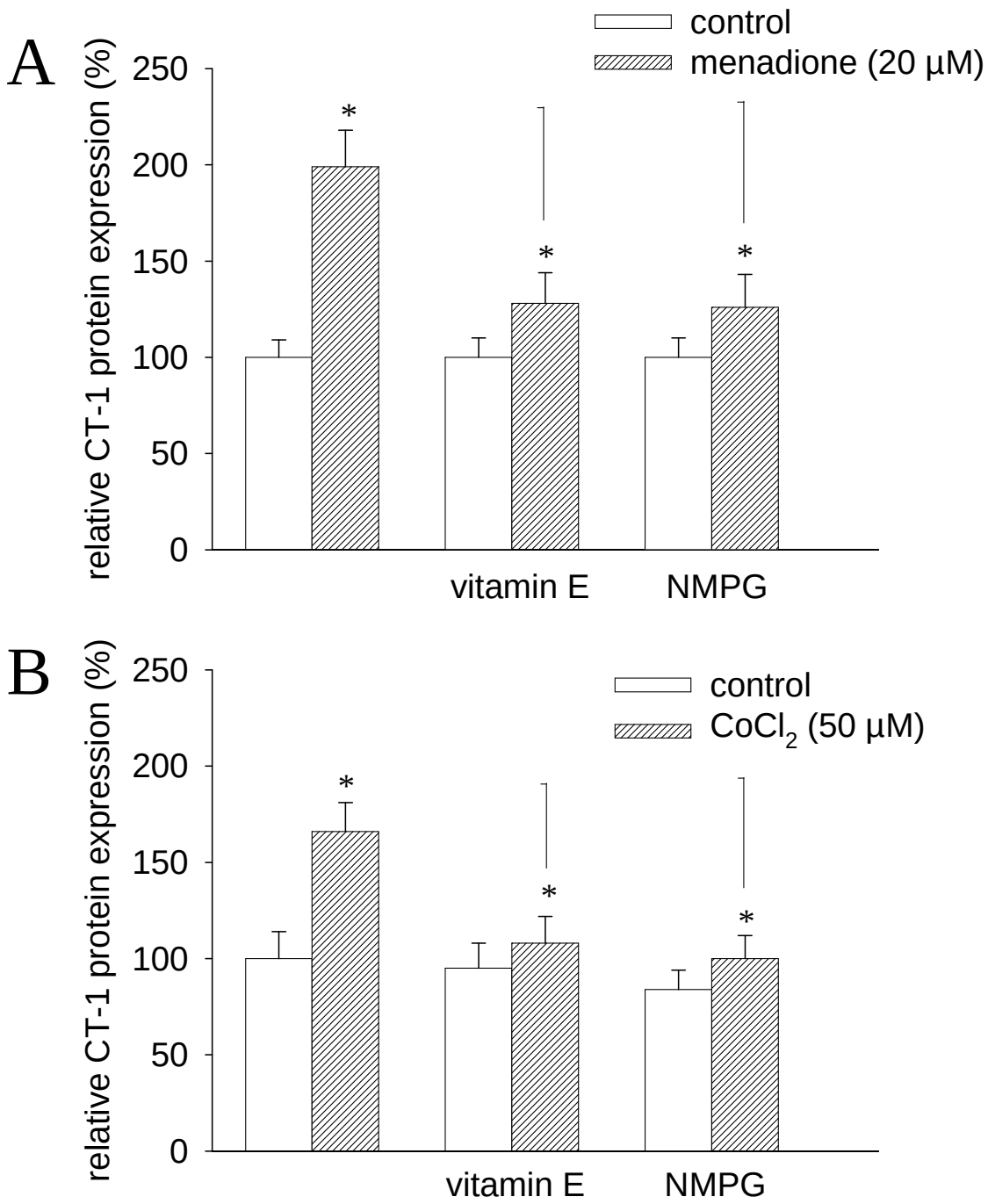
A
control
menadione (20 µM)
relative CT-1 protein expression (%)
250
200
150
100
50
0
*
*
*
vitamin E
NMPG
B
control
CoCl2 (50 µM)
relative CT-1 protein expression (%)
250
200
150
100
50
0
*
*
*
vitamin E
NMPG

Figure 7

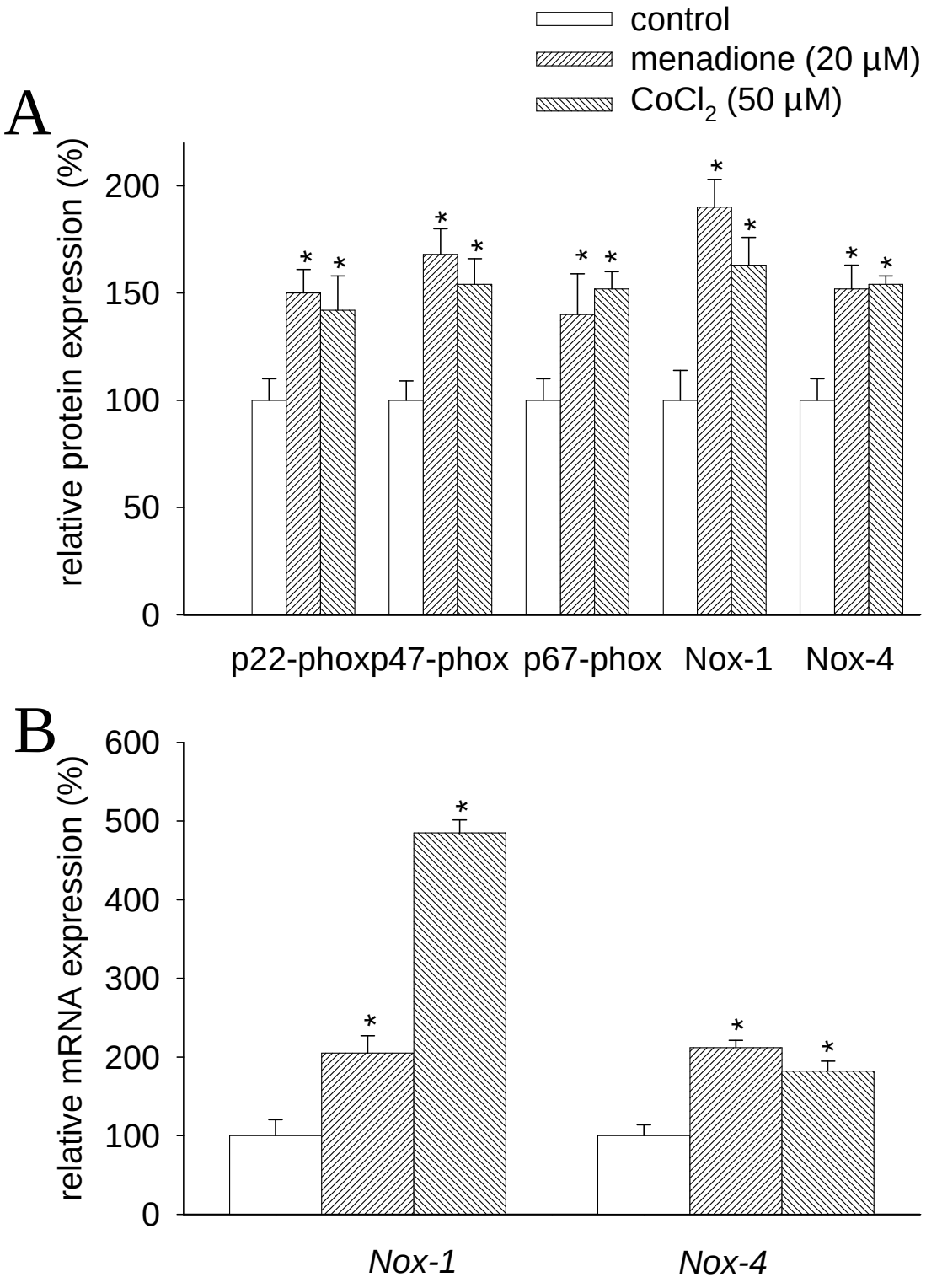
A
control
menadione (20 µM)
CoCl2 (50 µM)
relative protein expression (%)
0
50
100
150
200
p22-phox
p47-phox
p67-phox
Nox-1
Nox-4
B
relative mRNA expression (%)
0
100
200
300
400
500
600
Nox-1
Nox-4

Figure 8

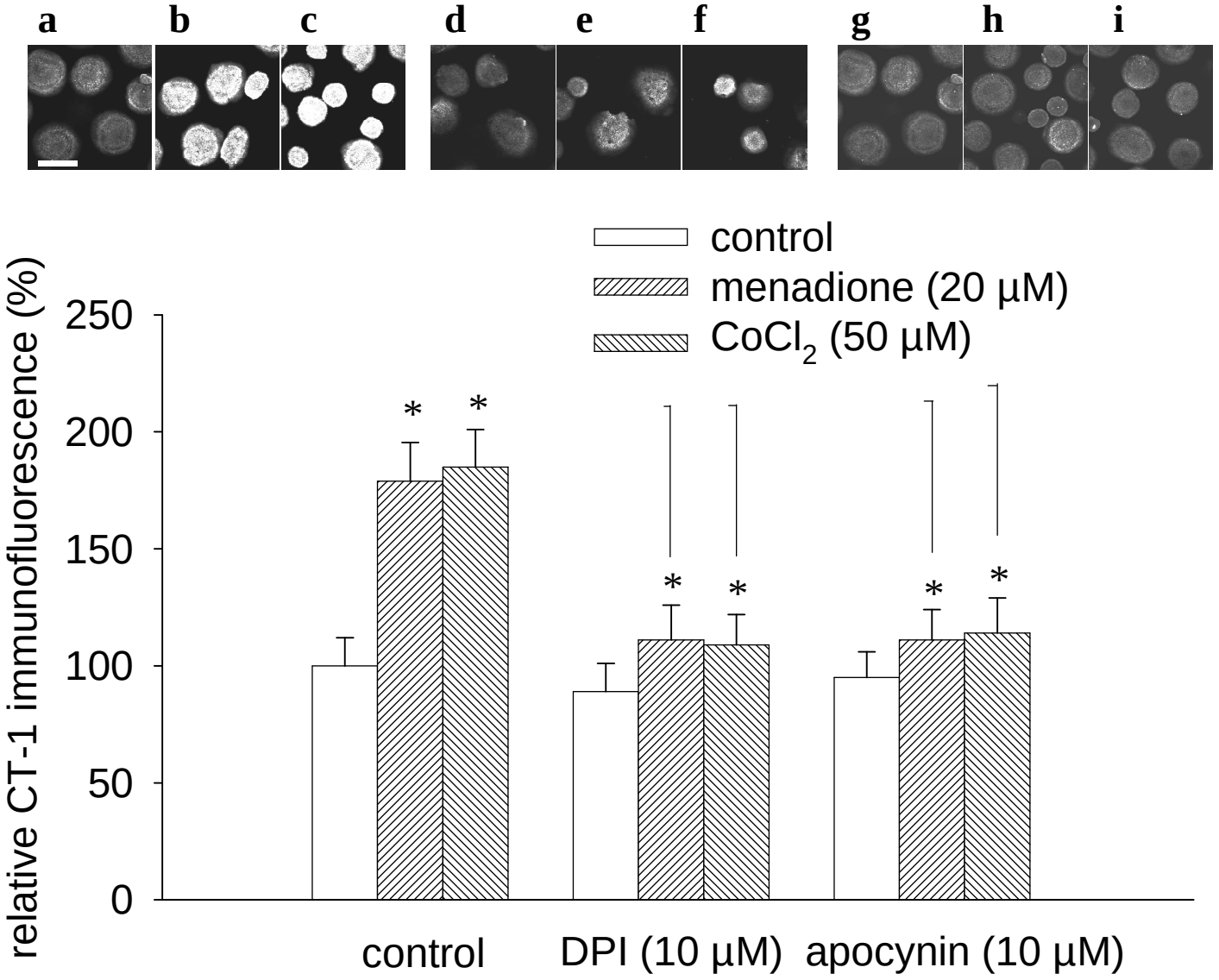
a
b
c
d
e
f
g
h
i
control
menadione (20 µM)
CoCl2 (50 µM)
relative CT-1 immunofluorescence (%)
250
200
150
100
50
0
*
control
DPI (10 µM)
apocynin (10 µM)

Figure 9

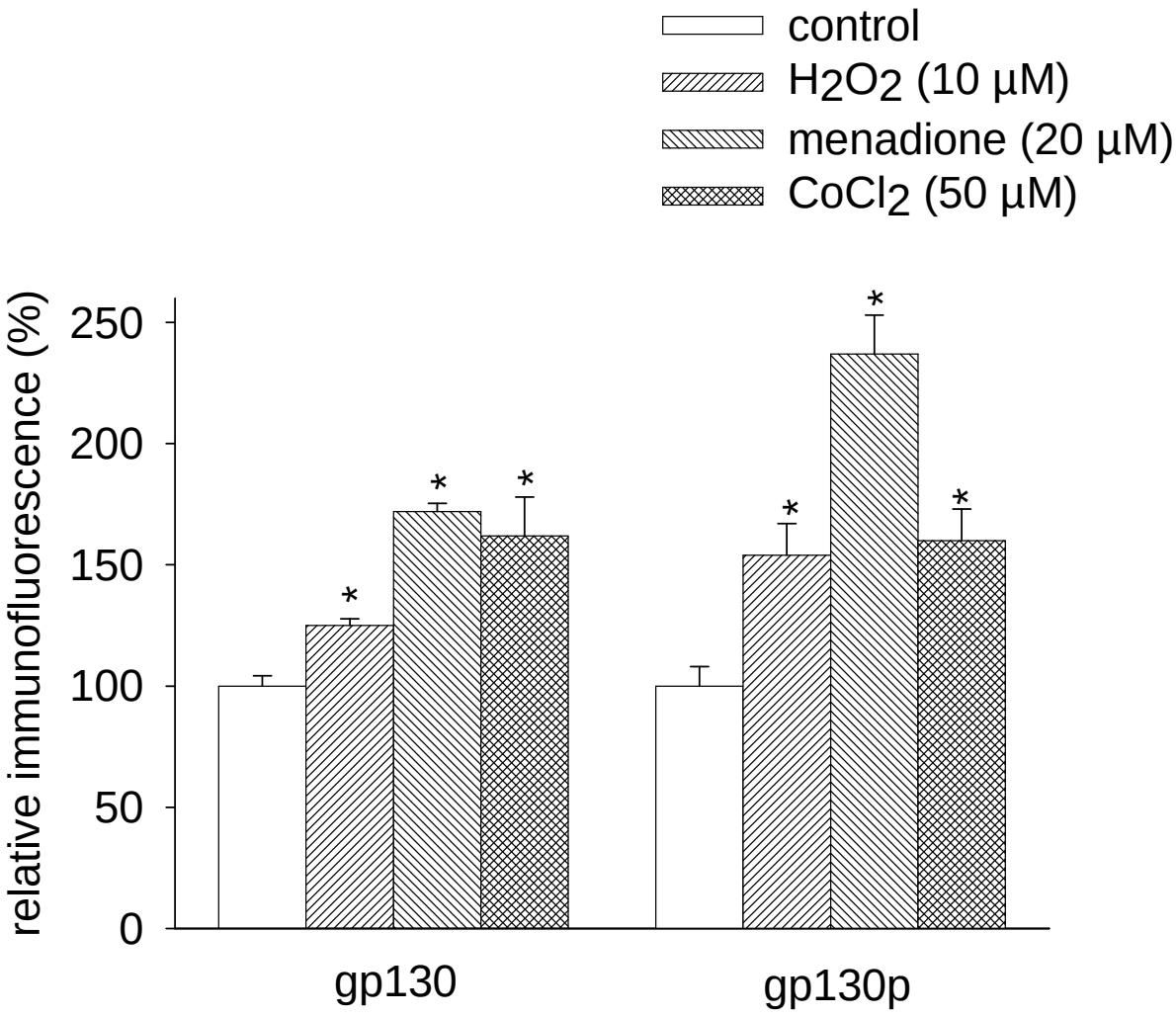
control
H2O2 (10 µM)
menadione (20 µM)
CoCl2 (50 µM)
relative immunofluorescence (%)
250
200
150
100
50
0
*
*
*
*
*
gp130
gp130p

Figure 10

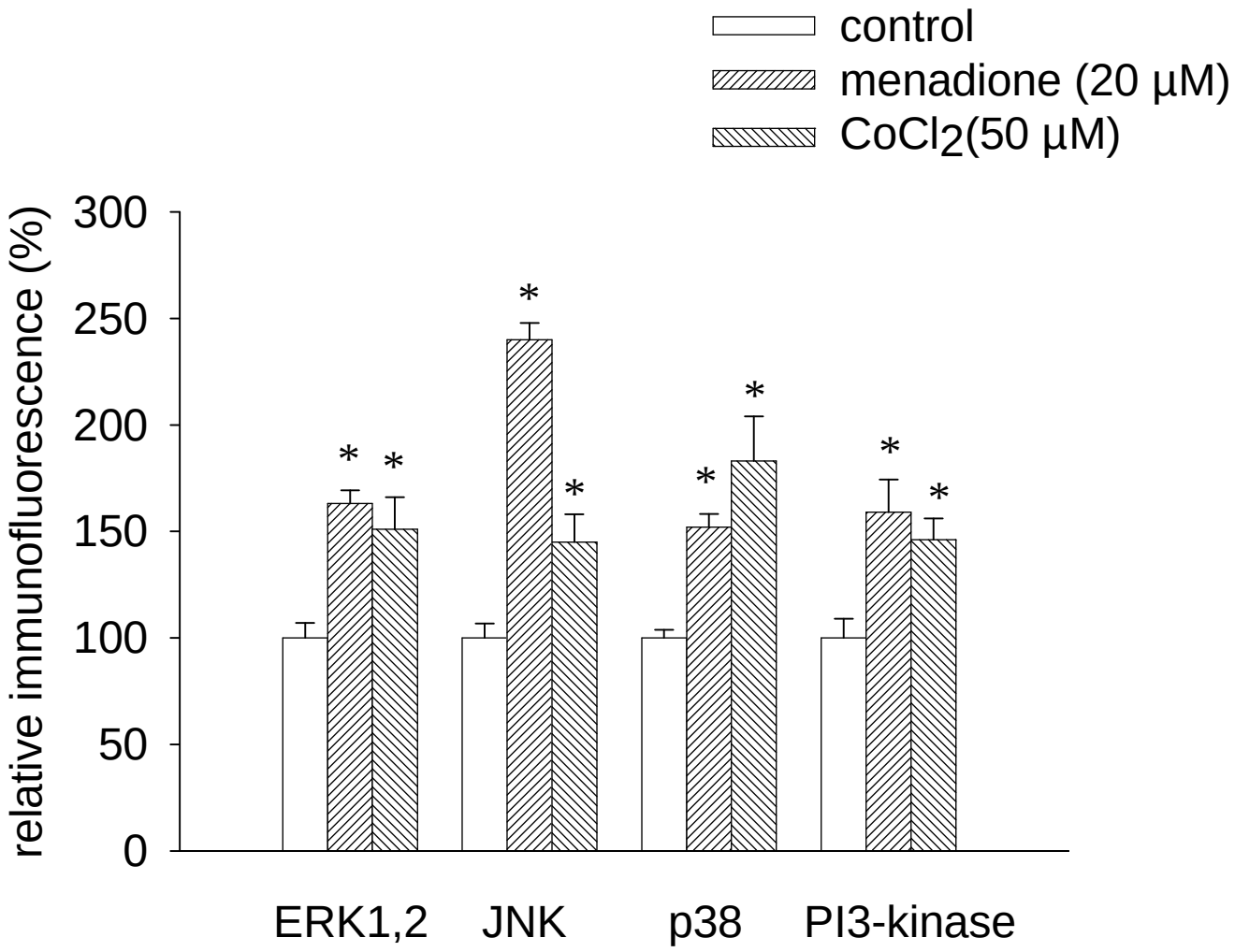
control
menadione (20 µM)
CoCl2(50 µM)
relative immunofluorescence (%)
300
250
200
150
100
50
0
*
ERK1,2
JNK
p38
PI3-kinase

Figure 11

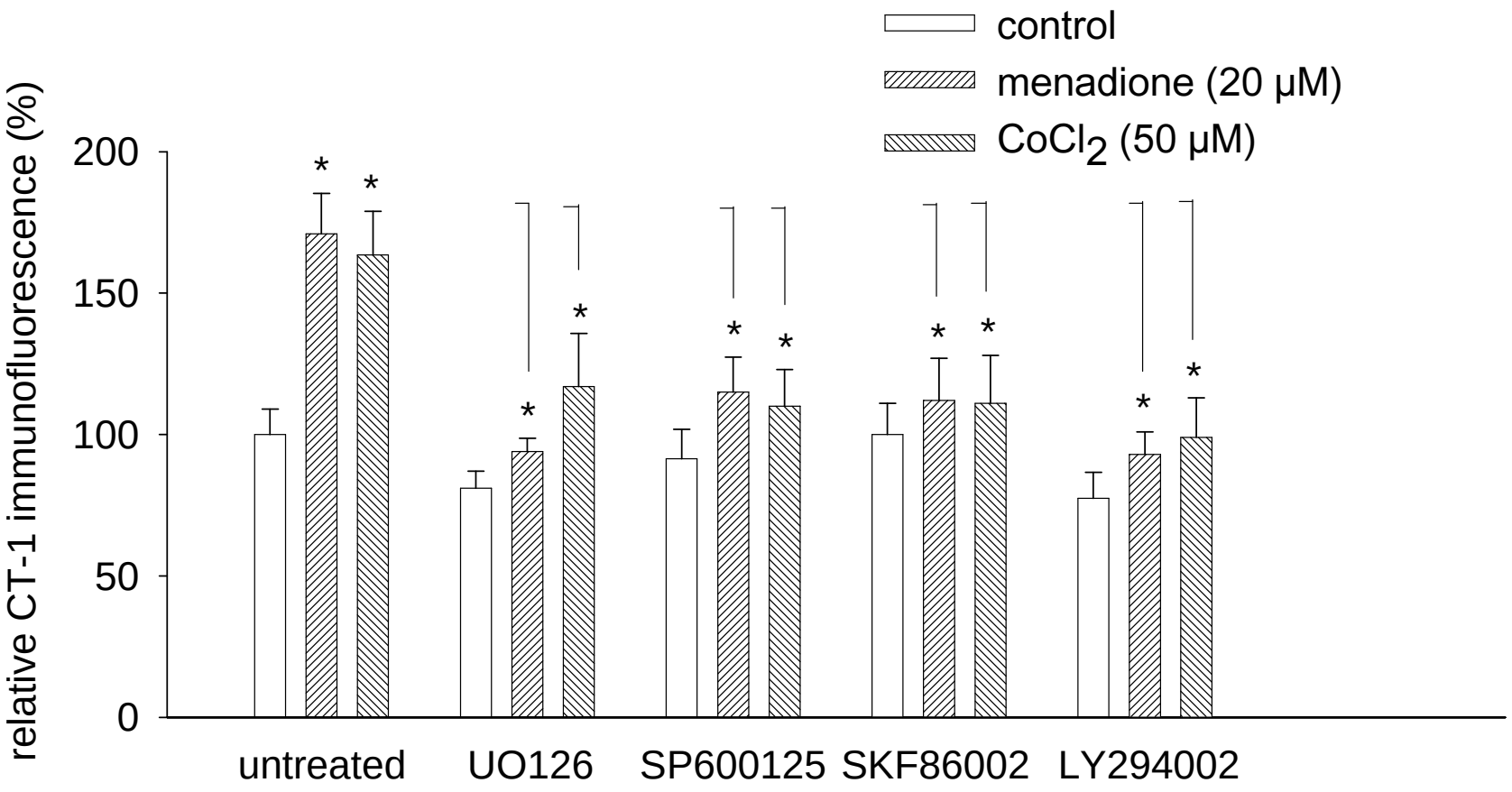
control
menadione (20 µM)
CoCl2 (50 µM)
relative CT-1 immunofluorescence (%)
200
150
100
50
0
*
untreated
UO126
SP600125
SKF86002
LY294002

Figure 12

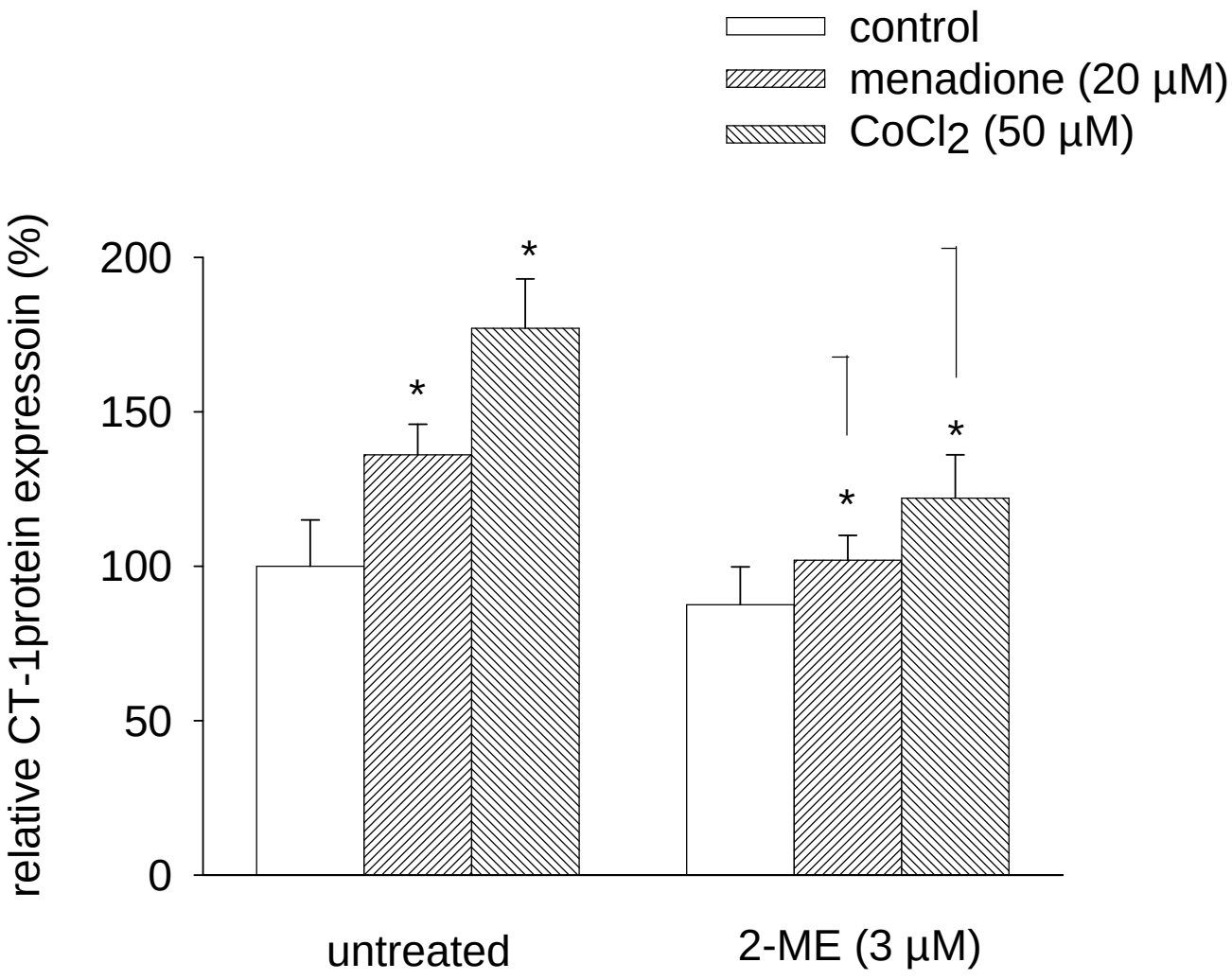
control
menadione (20 µM)
CoCl2 (50 µM)
relative CT-1protein expressoin (%)
200
150
100
50
0
*
*
*
*
untreated
2-ME (3 µM)

Figure 13*A,B*

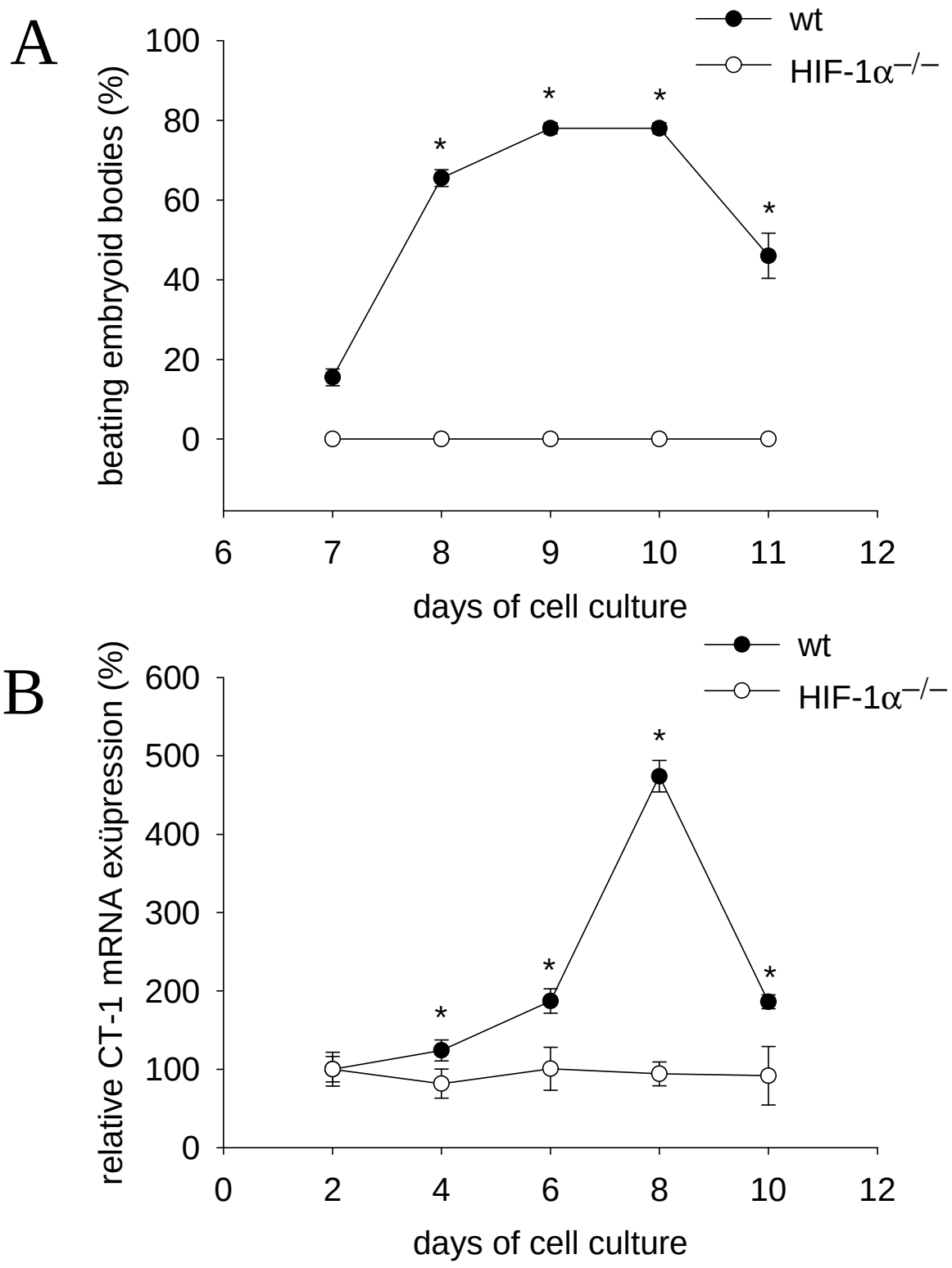
A
wt
HIF-1α−/−
beating embryoid bodies (%)
100
80
60
40
20
0
6
7
8
9
10
11
12
days of cell culture
B
wt
HIF-1α−/−
relative CT-1 mRNA exüpression (%)
600
500
400
300
200
100
0
0
2
4
6
8
10
12
days of cell culture

Figure 13*C*

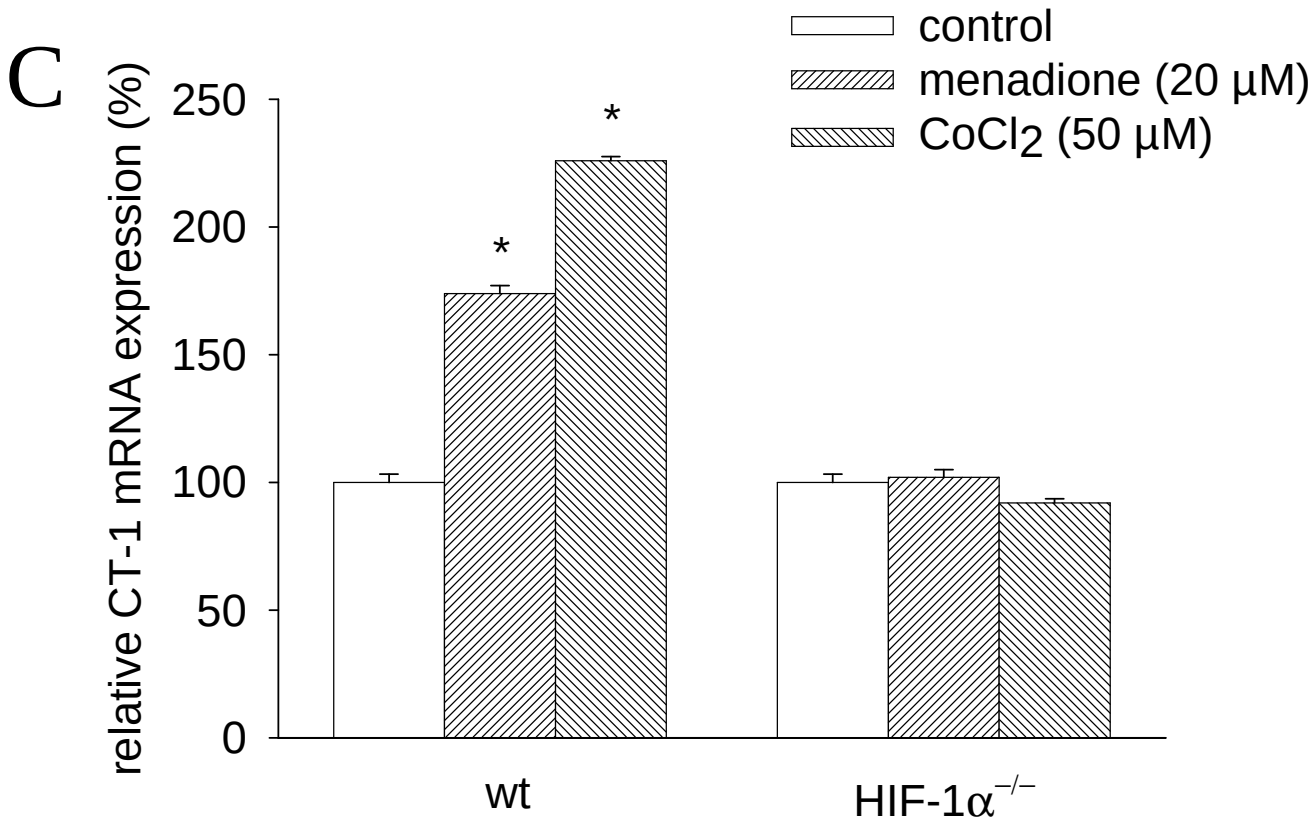
C
control
menadione (20 µM)
CoCl2 (50 µM)
relative CT-1 mRNA expression (%)
250
200
150
100
50
0
*
*
wt
HIF-1α−/−